An evolutionarily conserved protein CHORD regulates scaling of dendritic arbors with body size

Kohei Shimono[1], Kazuto Fujishima[2], Takafumi Nomura[1], Masayoshi Ohashi[1], Tadao Usui[1], Mineko Kengaku[1,2], Atsushi Toyoda[3], Tadashi Uemura[1*]

[1]Graduate School of Biostudies, Kyoto University, Kyoto 606-8501, Japan

[2]Institute for Integrated Cell-Material Sciences (WPI-iCeMS), Kyoto University Kyoto 606-8501, Japan.

[3]Center for Information Biology, National Institute of Genetics, Mishima, Shizuoka, Japan

Figure S1

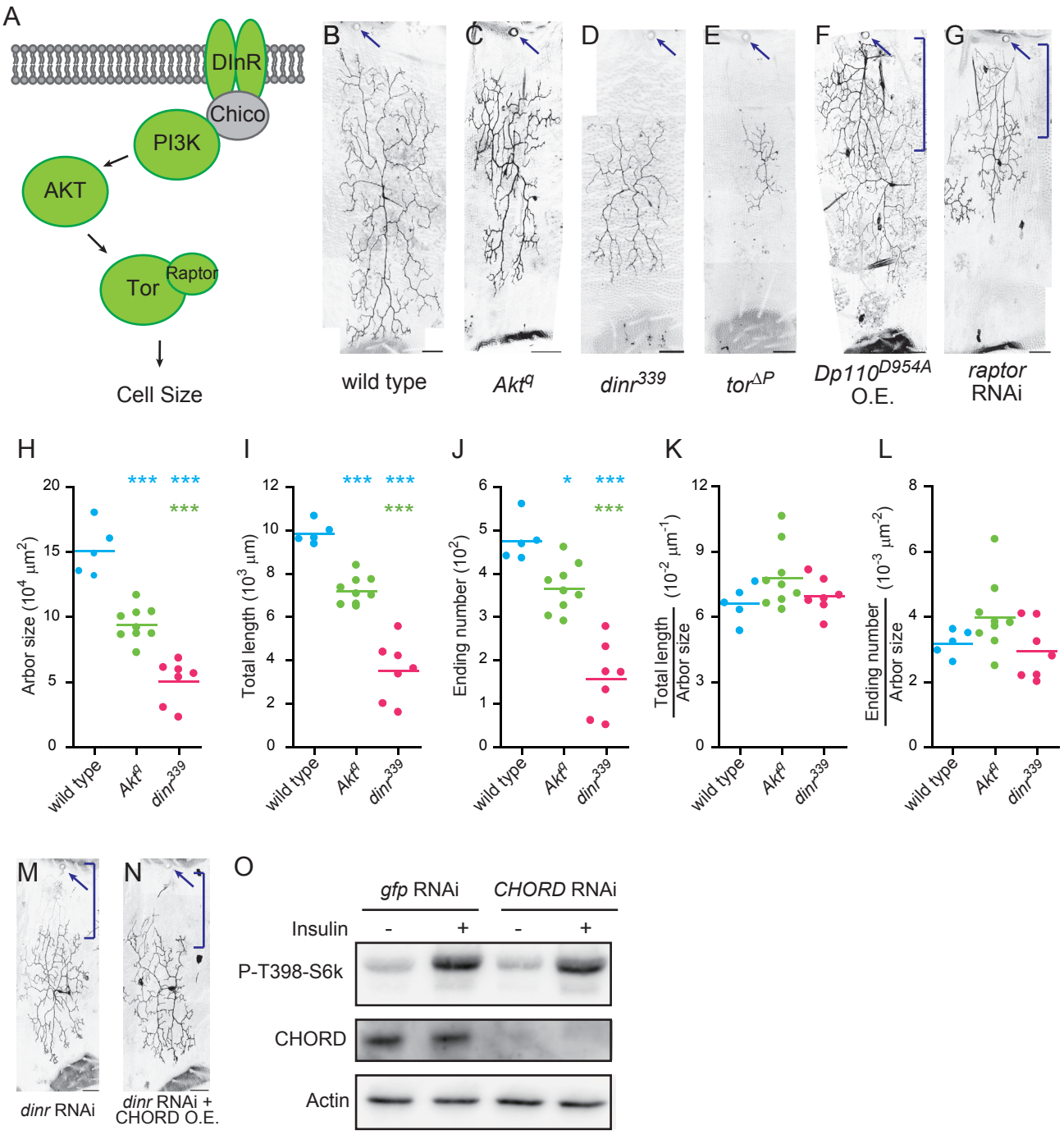
A
DInR
Chico
PI3K
AKT
Tor
Raptor
Cell Size
B
C
D
E
F
G
wild type
Akt^q
dinr^339
tor^ΔP
Dp110^D954A O.E.
raptor RNAi
H
I
J
K
L
Arbor size (10^4 µm^2)
Total length (10^3 µm)
Ending number (10^2)
Total length / Arbor size (10^-2 µm^-1)
Ending number / Arbor size (10^-3 µm^-2)
wild type
Akt^q
dinr^339
M
N
dinr RNAi
dinr RNAi + CHORD O.E.
O
gfp RNAi
CHORD RNAi
Insulin
P-T398-S6k
CHORD
Actin

Figure S2

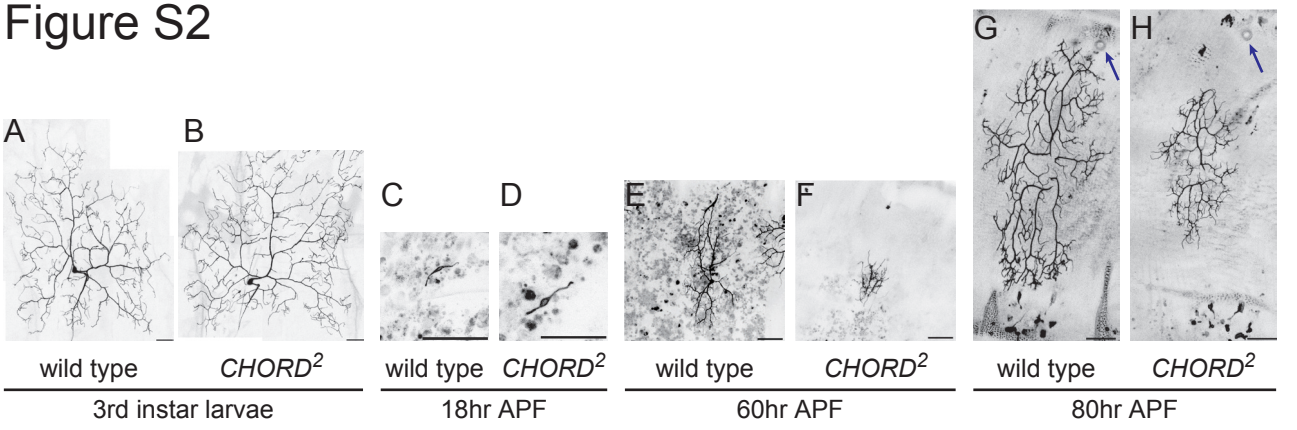
A
B
C
D
E
F
G
H
wild type
CHORD2
wild type
CHORD2
wild type
CHORD2
wild type
CHORD2
3rd instar larvae
18hr APF
60hr APF
80hr APF

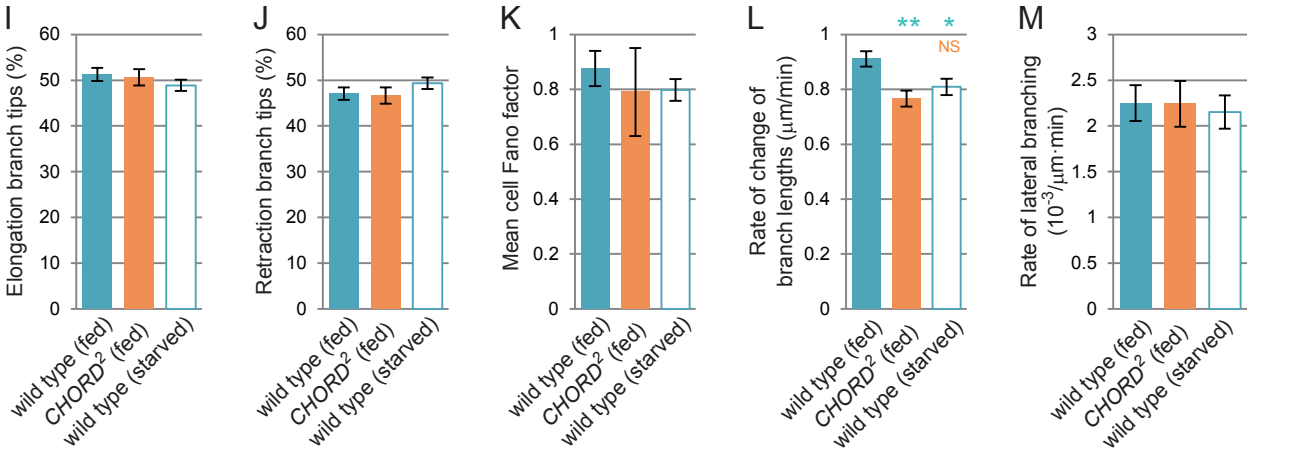
I
Elongation branch tips (%)
J
Retraction branch tips (%)
K
Mean cell Fano factor
L
Rate of change of branch lengths (μm/min)
**
*
NS
M
Rate of lateral branching (10-3/μm·min)
wild type (fed)
CHORD2 (fed)
wild type (starved)

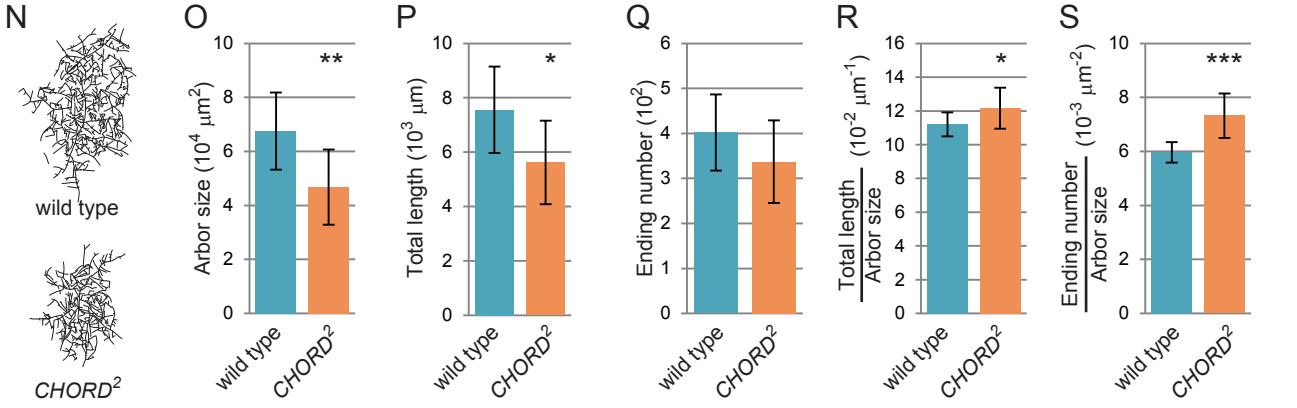
N
wild type
CHORD2
O
Arbor size (10^4 μm^2)
P
Total length (10^3 μm)
Q
Ending number (10^2)
R
Total length / Arbor size (10^-2 μm^-1)
S
Ending number / Arbor size (10^-3 μm^-2)
**
*
*
***
wild type
CHORD2

Figure S3

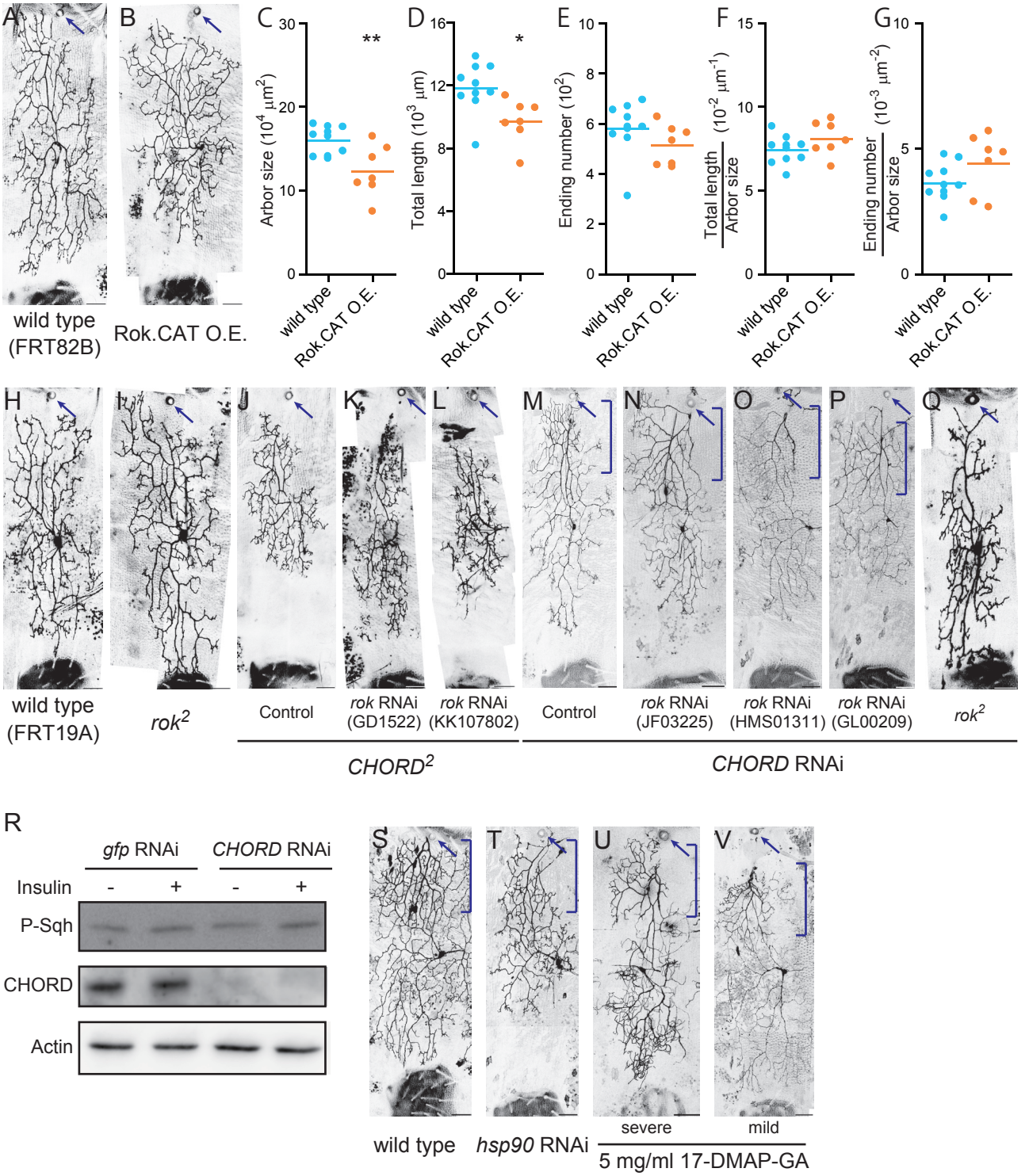
A
B
C
D
E
F
G
wild type (FRT82B)
Rok.CAT O.E.
Arbor size (10^4 µm^2)
Total length (10^3 µm)
Ending number (10^2)
Total length / Arbor size (10^{-2} µm^{-1})
Ending number / Arbor size (10^{-3} µm^{-2})
**
*
wild type
Rok.CAT O.E.
H
I
J
K
L
M
N
O
P
Q
wild type (FRT19A)
rok2
Control
rok RNAi (GD1522)
rok RNAi (KK107802)
Control
rok RNAi (JF03225)
rok RNAi (HMS01311)
rok RNAi (GL00209)
rok2
CHORD2
CHORD RNAi
R
gfp RNAi
CHORD RNAi
Insulin
-
+
-
+
P-Sqh
CHORD
Actin
S
T
U
V
wild type
hsp90 RNAi
severe
mild
5 mg/ml 17-DMAP-GA

Figure S4

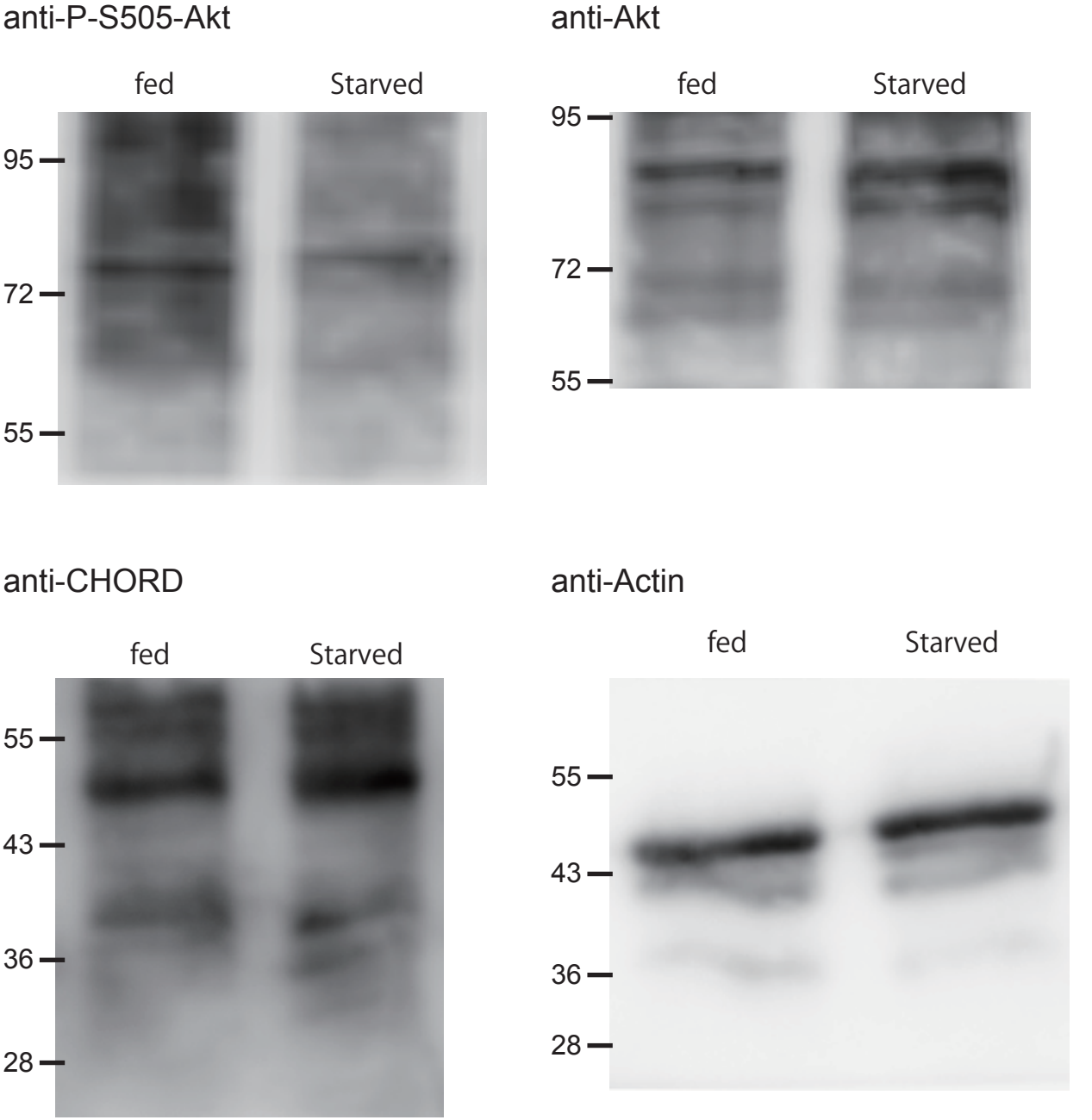
anti-P-S505-Akt
fed
Starved
95
72
55
anti-Akt
fed
Starved
95
72
55
anti-CHORD
fed
Starved
55
43
36
28
anti-Actin
fed
Starved
55
43
36
28

Supplementary Figure S1. Mutant neurons of the IIS signaling pathways showed dendrite "undergrowth".

(A) A "bare bones" schematic diagram of the IIS pathway. (B-G) Representative images of MARCM clones of the wild-type neuron, v'ada, (B), *Akt* mutant neuron (C; Akt^{q}), *drosophila insulin receptor* mutant neuron (D; $dinr^{339}$), and *tor* mutant neuron (E; Tor^{deltaP}), the wild-type neurons overexpressing a dominant negative form of PI3K (F; $Dp110^{D954A}$ O.E.), and *raptor* knockdown neurons (G; *raptor* RNAi). Note that dendrites of adjacent da neurons, ldaA/ldaA-like, were also labeled in F and G (indicated by bracket) [1]. In these and subsequent images of the neurons, posterior is to the right and dorsal is at the top, and arrows indicate spiracles. Scale bars, 50 μm.

(H-L) Quantitative analysis of dendritic-arbor patterns. (H) Dendritic arbor size. (I) Total length of dendritic branches. (J) The number of endings of dendritic branches. (K and L) The branch density: total length/arbor size (K) and ending number/arbor size (L). Arrows indicate spiracles. *$p < 0.05$, **$p < 0.01$, and ***$p < 0.001$. (M and N) Representative images of the *dinr* knockdown neurons and the knockdown neurons in which CHORD was overexpressed, respectively. Overexpression of CHORD didn't rescue the undergrowth phenotype of the *dinr* knockdown neurons. (O) S2 cells were incubated with dsRNA against the indicated genes for 3 days and then treated with or without 10 μg/ml insulin for 30 min before harvesting. Cell lysates were then analyzed by immunoblotting for phosphorylated S6K (Thr398), which is a readout of IIS/TORC1 pathways, CHORD, and actin.

Supplementary Figure S2. Quantitative analysis of dendrite dynamics of real neurons and morphological features of model neurons

(A-H) Representative images of MARCM clones of the wild-type (A, C, E, and G) and *CHORD*^{2} mutant neurons (B, D, F and H) at developmental stages indicated. Images were obtained at 3rd instar larval stage (A and B), 18hr APF (C and D), 60 hr APF (E and F), and 80 hr APF (G and H). After larval dendrites were pruned, primary branches emerged from the v'ada cell bodies (C). *CHORD* mutant neurons underwent pruning and subsequent regeneration of branches along the normal timeline (D). At 60 hr APF onwards, the arbor undergoes a persistent increase in complexity and size with generation of higher-order branches (E-H). Scale bars, 50 μm.

(I-M) Quantification of dendritic dynamics of the wild-type under the fed or starved condition and *CHORD*^{2} mutant neurons under the fed condition (see also Movie S1-S3). (I and J) Frequencies of elongating (I) and retracting (J) terminal branches, respectively. (K) Mean cell Fano factor. (L) The rate of branch–length changes (absolute values) of terminal branches. (M) The rate of lateral branching. n=78, 55, and 63 terminal branches from 3 cells of the wild type under fed or starved condition and *CHORD*^{2}, respectively. Data are presented as means ± standard error (SE). *$p < 0.05$ and **$p < 0.01$.

(N-S) Dendritic arbors of model neurons. (N) Representative images of the wild-type and *CHORD* mutant neurons in silico under the fed condition. (O-S) Quantifications. (O) Dendritic arbor size. (P) Total length of dendritic branches. (Q) The number of branch endings. (R and S) The branch density: total length/arbor size (R) and ending number/arbor size (S). Data are presented as means ± standard deviation (SD). *$p < 0.05$, **$p < 0.01$, and ***$p < 0.001$.

Supplementary Figure S3. Examination of the involvement of Rok and HSP90 in

scaling of dendritic arbors.

It has been reported in animals that CHORD together with HSP90 negatively regulates Rho kinase (Rok) activity [2]. If this molecular function of CHORD plays a critical role in scaling of dendritic arbors, we suspected that Rok would be hyperactivated in *CHORD* mutant or knockdown cells, hence causative of the miniature phenotype, and that inhibition of HSP90 function may reproduce the *CHORD* mutant-like miniature phenotype. To examine these possibilities, we addressed the following questions: Does overexpression of Rok[CA], the constitutively active form of Rok [3], generate miniature dendritic arbors (A-G)? Is the *CHORD* miniature phenotype suppressed by a loss-of-function mutation of *Rok* or knockdown of *Rok* (H-Q)? Is the Rok activity upregulated by a *CHORD* knockdown in S2 cells (R)? Does knockdown of *hsp90* or application of a HSP90 inhibitor cause a miniature-like phenotype (S-V)? Answers to all of these questions were negative as described below:

(A-G) Representative images of MARCM clones of the wild-type neurons (A) and the wild-type neurons overexpressing Rok[CA] (B). (C-E) Quantitative analysis of dendritic-arbor patterns. (C) Dendritic arbor size. (D) Total length of dendritic branches. (E) The number of endings of dendritic branches. (F and G) The branch density: total length/arbor size (F) and ending number/arbor size (G). Rok[CA] overexpression did not increase the branch density. *$p < 0.05$ and **$p < 0.01$. Throughout this figure, arrows indicate spiracles and scale bars equal 50 μm.

(H-Q) Representative images of wild-type neurons (H) and *rok* mutant neurons (I), which showed neither dramatic miniature nor undergrowth phenotype. (J-L) Knockdown of *Rok* in *CHORD* mutant neurons (K and L) and control (J). (M-Q) Double knockdown of *rok* and *CHORD* (N-P), *rok* mutant clone in which *CHORD* was

knocked down (Q), and control (M). The *CHORD* miniature phenotype was not noticeably suppressed by knockdown or loss-of-function of *Rok*. Note that dendrites of adjacent da neurons, ldaA/ldaA-like, were also labeled (indicated by bracket) [1].

(R) Lysates of S2 cells were analyzed by immunoblotting for the phosphorylated form of Spaghetti squash (Sqh: the regulatory light chain of nonmuscle myosin) that is a readout of Rok activity, CHORD, and actin. The membrane used in Figure S1O was reblotted with anti-phospho-Sqh antibody. The level of phospho-Sqh (P-Sqh) was not affected by knockdown of *CHORD*.

(S-V) (S) The wild-type neuron. (T) An example of neurons in which *hsp90* was knocked down during pupal stages. We employed this temporal knockdown because knocking down *hsp90* throughout larval stages killed neurons. (U and V) The wild-type neurons to which HSP90 inhibitor 17DMAP-GA (InvivoGen) was administered (injection of 5 mg/ml solution). The effects of the inhibitor on dendrite formation were quite variable. Dendrites of adjacent da neurons, ldaA/ldaA-like, are indicated by brackets [1].

Supplementary Figure S4. Cropped immunoblots from Figure 4K are shown in full.

Supplementary Video S1. Recording of dendritic dynamics of the wild-type neuron under the fed condition

A time-lapse recording of dendritic branches of the wild-type neuron under the fed condition between 70 hr and 74 hr APF, taken with a 2 μm Z-step and at 2 min intervals for total 1 hr. See the legend of Figure 1 for explanations. Scale bar, 50 μm.

Supplementary Video S2. Recording of dendritic dynamics of the *CHORD* mutant neuron

A time-lapse recording of dendritic branches of a *CHORD* mutant neuron under the fed condition. See the legend of Video S1 for other explanations.

Supplementary Video S3. Recording of dendritic dynamics of the wild-type neuron under the starved condition

A time-lapse recording of dendritic branches of the wild-type neuron under the starved condition. See the legend of Video S1 for other explanations.

Supplementary Table S1. List of Drosophila strains

Figure	Abbreviation	Genotype
1B, 1E, 1F, 2B, S1B, S2A, S2C, S2E, S2G, S3A	wild type	*Gal4$^{5-40}$ UAS-Venus:pm SOP-FLP#42/+; +/+; FRT82B/FRT82B tubPGal80*
2C, 3A, 3B, S2B, S2D, S2F, S2H, S3J	*CHORD^{2}*	*Gal4$^{5-40}$ UAS-Venus:pm SOP-FLP#42/+; +/+; FRT82B CHORD^{2}/FRT82B tubPGal80*
2D	rescue	*Gal4$^{5-40}$ UAS-Venus:pm SOP-FLP#42/+; CHORD genomic fragment/+; FRT82B CHORD^{2}/FRT82B tubPGal80*
4A, S3H	wild type	*FRT19A/FRT19A tubPGal80; Gal4$^{109(2)80}$ UAS-mCD8:GFP SOP-FLP#73/CyO*
4B	*rictor$^{\Delta 2}$*	*FRT19A rictor$^{\Delta 2}$/FRT19A tubPGal80; Gal4$^{109(2)80}$ UAS-mCD8:GFP SOP-FLP#73/CyO*
4C	*rictor$^{\Delta 2}$* + CHORD O.E.	*FRT19A rictor$^{\Delta 2}$/FRT19A tubPGal80; Gal4$^{109(2)80}$ UAS-mCD8:GFP SOP-FLP#73/UAS-CHORD*
S1C	*Akt[q]*	*Gal4$^{5-40}$ UAS-Venus:pm SOP-FLP#42/+; +/+; FRT82B Akt^{q}/FRT82B tubPGal80*
S1D	*dinr[339]*	*Gal4$^{5-40}$ UAS-Venus:pm SOP-FLP#42/+; +/+; FRT82B dinr^{339}/FRT82B tubPGal80*
S1E	*tor[deltaP]*	*Gal4$^{5-40}$ UAS-Venus:pm SOP-FLP#42/+; tor^{deltaP} FRT40A/tubPGal80 FRT40A*
S1F	*Dp110[D954A]* O.E.	*Gr28b.c.Gal4 UAS-mCD8:GFP/UAS-Dp110[D954A]*
S1G	*raptor* RNAi	*Gr28b.c.Gal4 UAS-mCD8:GFP/+; TRiP(HMS00124)/+*
S3B	Rok.CAT O.E.	*Gal4$^{5-40}$ UAS-Venus:pm SOP-FLP#42/+; UAS-Rok.CAT48.2/+; FRT82B CHORD^{2}/FRT82B tubPGal80*
S3I	*rok^{2}*	*FRT19A rok^{2}/FRT19A tubPGal80; Gal4$^{109(2)80}$ UAS-mCD8:GFP SOP-FLP#73/+*
S3K	*rok* RNAi in *CHORD^{2}* (GD1522)	*Gal4$^{5-40}$ UAS-Venus:pm SOP-FLP#42/+; (GD1522)v3793/+; FRT82B CHORD2/FRT82B tubPGal80*
S3L	*rok* RNAi in *CHORD^{2}* (KK107802)	*Gal4$^{5-40}$ UAS-Venus:pm SOP-FLP#42/+; (KK107802)VIE-260B/+; FRT82B CHORD^{2}/FRT82B tubPGal80*
S3M	*CHORD* RNAi	*Gr28b.c.Gal4 UAS-mCD8:GFP/UAS-CHORD IR#1; UAS-dcr2/+*
S3N	*CHORD* & *rok* RNAi (JF03225)	*Gr28b.c.Gal4 UAS-mCD8:GFP/UAS-CHORD IR#1; TRiP(JF03225)/+*
S3O	*CHORD* & *rok* RNAi (HMS01311)	*Gr28b.c.Gal4 UAS-mCD8:GFP/UAS-CHORD IR#1; TRiP(HMS01311)/+*
S3P	*CHORD*& *rok* RNAi (GL00209)	*Gr28b.c.Gal4 UAS-mCD8:GFP/UAS-CHORD IR#1; TRiP(GL00209)/+*
S3Q	*CHORD* RNAi in *rok^{2}*	*FRT19A rok^{2}/FRT19A tubPGal80; Gal4$^{109(2)80}$ UAS-mCD8:GFP SOP-FLP#73/UAS-CHORDIR#1*
S3S	wild type	*Gr28b.c. UAS-mCD8:GFP/+; UAS-tubPGal80ts/UAS-mCD8.mRFP*
S3T	*hsp90* RNAi	*Gr28b.c. UAS-mCD8:GFP/+; UAS-tubPGal80^{ts}/TRiP(HMS00899)*
S3U, S3V	5 mg/ml 17-CMAP-GA	*Gr28b.c. UAS-mCD8:GFP/+*

Supplementary Table S2. List of transposon insertion strains isolated from genetic screen

DGRC number	ID Number	Gene Symbol[(a)]	CG Number	Phenotypes
140015	LL00066	*heph*	*CG31000*	undergrowth
140052	LL00232	*Gyc-89Db*	*CG14886*	undergrowth
140161	LL00779	*l(3)01239, CG7839*	*CG6302, CG7839*	undergrowth
140293	LL01235	*TfIIFalpha, CG1024*	*CG10281, CG1024*	undergrowth
140294	LL01237	*pum*	*CG9755*	undergrowth
140686	LL02779	*Rel, Nmdmc*	*CG11992, CG18466*	undergrowth
140949	LL06331	*Mbs*	*CG32156*	undergrowth
141022	LL03277	*krz, mod*	*CG1487, CG2050*	miniature[(b)]
141154	LL03972	*sda*	*CG5518*	undergrowth
141180	LL04133	*Spase22-23, Acp95EF*	*CG5677, CG17924*	miniature[(b),(c)]
141193	LL04168	*Bub3, CAP-D2*	*CG7581, CG1911*	undergrowth
141209	LL04239	*Tor*	*CG5092*	undergrowth
141303	LL04611	*ModSP*	*CG31217*	miniature[(b),(c)]
141361	LL04839	*CG11815, CG1139*	*CG11815, CG1139*	undergrowth
141470	LL01162	*SMC1*	*CG6057*	undergrowth
141547	LL05277	*sar1*	*CG7073*	undergrowth
141596	LL05452	*Rab11*	*CG5771*	undergrowth
141628	LL05552	*Trn-SR*	*CG2848*	undergrowth
141785	LL06325	*Pect , CG16972*	*CG5547, CG16972*	undergrowth
141821	LL06541	*btsz*	*CG33555*	undergrowth
141889	LL03660	*pasha*	*CG1800*	undergrowth
141929	LL06861	*exba*	*CG2922*	undergrowth

(a) Genes located nearby *piggyBac* insertion are listed.

(b) These strains belong to same lethal complementation group.

(c) Whole-genome sequences of these strains were determined and they have a 1bp deletion in the *CHORD/morgana* gene.

Supplementary Table S3. Parameters used in computer simulation

Parameter		Value	
Abbreviation	Explanation	wild-type	*CHORD*^{2}
L	Length of unit segment	0.9 μm	0.75 μm
X	Width of the space	600 μm	
Y	Height of the space	600 μm	
T	Calculation step	3000 min	
pe	Probability of elongation	0.51	
pr	Probability of retraction	0.47	
pl[(a)]	Probability of lateral branching per segment	0.002	0.0017

(a) Note that pl is calculated by multiplying the average value in Figure 4F by length of unit segment (L).

Supplemental References

1 Shimono, K. *et al.* Multidendritic sensory neurons in the adult Drosophila abdomen: origins, dendritic morphology, and segment- and age-dependent programmed cell death. *Neural Dev* **4**, 37, doi:10.1186/1749-8104-4-37 (2009).

2 Ferretti, R. *et al.* Morgana/chp-1, a ROCK inhibitor involved in centrosome duplication and tumorigenesis. *Dev Cell* **18**, 486-495, doi:10.1016/j.devcel.2009.12.020 (2010).

3 Simões, S. e. M. *et al.* Rho-kinase directs Bazooka/Par-3 planar polarity during Drosophila axis elongation. *Dev Cell* **19**, 377-388, doi:10.1016/j.devcel.2010.08.011 (2010).